

# Dynamics of a barrier discharge at high overvoltage

V. N. Khudik,<sup>a)</sup> V. P. Nagorny, and A. Shvydky  
*Plasma Dynamics, Corp., 417 E. 8 Mile Rd, Hazel Park, Michigan 48030*

(Received 8 May 2003; accepted 25 August 2003)

The dynamics of a strong barrier discharge is investigated analytically in the simplest model that still keeps the essential discharge features. It is shown that at high overvoltage, the discharge develops into the ionizing wave moving from the anode toward the cathode. The velocity of this wave is found to be controlled mainly by the charge production rate in the cathode fall region and can considerably exceed the characteristic ion velocity. The influence of the capacitor formed by the dielectric layers on the discharge dynamics is analyzed. It is shown that, depending on the magnitude of the capacitance, two qualitatively different charging regimes exist. © 2003 American Institute of Physics. [DOI: 10.1063/1.1618921]

## I. INTRODUCTION

Interest in barrier discharges is sustained by their wide application in different areas including environmental<sup>1</sup> and industrial.<sup>2,3</sup> The parameter  $pD$  in these discharges ranges from a few to several hundred Torr cm which likens them to glow discharges. But in contrast to the latter, barrier discharges have a capacitive limiter to the current and are operated under ac voltage (with frequency from several kHz up to several hundred kHz). The inherently transient nature of the barrier discharge makes a systematic study of its dynamics important.

In recent years, a number of computer simulations were performed to investigate quite complicated models of the barrier discharge.<sup>4–16</sup> Taking into account a great diversity of physical processes, they are capable of answering many practically important questions. Being a convenient tool for verifying hypotheses, they are also quite useful in developing analytical theories. First, an analytical study of barrier discharges considers a very weak discharge, when the distortion of the electric field in the gas gap can be neglected.<sup>17</sup> The ideas developed in this work helped to solve some problems related to the operation of the plasma display panels. In this article, we consider the opposite case when the discharge is very strong and the distortion of the electric field is crucial.

The geometry of barrier discharges can be quite complicated either due to the complexity of the discharge cell geometry as in the case of plasma display panels<sup>6,7,16</sup> or due to complexity of the spatial structure of the discharge.<sup>18,19</sup> To avoid geometrical aspects of the problem, we present a one-dimensional analytical treatment of barrier discharges initiated by a high applied voltage. We restrict our consideration to the case when the discharge gap is filled by pure noble gas, and use the simplest hydrodynamic model that still keeps the essential features of the discharge dynamics. Despite simplifications, our analytical approach provides insight into the interplay of different processes in barrier discharges.

The plan of this article is as follows. In Sec. II, we qualitatively explain the mechanism controlling the dis-

charge dynamics, and show that at high overvoltage the discharge develops into an ionizing wave (somewhat similar to ionizing potential wave studied in the theory of streamers),<sup>20–22</sup> whose velocity is determined primarily by the charge production rate in the cathode fall (CF) region. This wave moves from the anode toward the cathode, resulting in contraction of the CF region and increasing the electric field within this region. Then, in Sec. III using a “step-like” approximation for the electric field, we obtain the basic equations for wave parameters. In Sec. IV, we investigate the propagation of the ionizing wave in the case when electrodes are not covered with a dielectric, and point out two qualitatively different regimes: A fast regime of the wave propagation and a slow one. The structure of the ionizing wave and the charge and plasma distributions in the gap are considered in Sec. V. The influence of the capacitance of the dielectric layers on the discharge dynamics is considered in Sec. VI. Depending on the magnitude of this capacitance, quite different types of discharges are found. In Sec. VII, we discuss the applicability and some generalizations of the results. Lastly, in Sec. VIII, we make several concluding remarks.

## II. QUALITATIVE CONSIDERATION

We will consider a single discharge pulse in the gas gap between the plane electrodes covered by dielectric layers (see Fig. 1). Let us recall that barrier discharges are operated at such values of parameter  $pD$  at which electron avalanche is controlled by the secondary emission of electrons from the cathode surface. Therefore, the breakdown voltage in our system is determined from the well known Townsend condition,

$$\Delta_T \equiv \gamma [e^{\alpha(E)L} - 1] - 1 = 0, \quad (1)$$

where  $\alpha$  is the Townsend ionization coefficient,  $\gamma$  is the secondary electron emission coefficient,  $E$  is the electric field in the gap, and  $L$  is the gas gap length. In the general case, the parameter  $\Delta_T$  can be a measure of how far the system is from the breakdown. It is equal to the number of extra ions created in the gap by the electron avalanche which results from one

<sup>a)</sup>Electronic mail: vkhudik@plasmadynamics.com

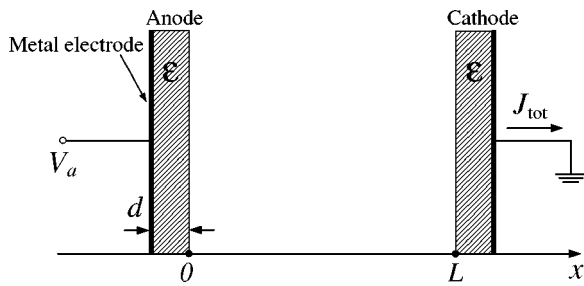


FIG. 1. Basic geometry.

ion striking the cathode; hence, the growth rate of the positive charge in the gap  $Q$  (per unit electrode area) is given by

$$\dot{Q} = \Delta_T j_{ic}, \tag{2}$$

where the dot means  $t$  derivative and  $j_{ic}$  is the ion component of the current density to the cathode. When the applied voltage  $V_a < V_{br}$ , the derivative  $\dot{Q} < 0$  and small amount of the initial seed charge vanishes without initiating a discharge. When the applied voltage is slightly higher than the breakdown voltage (i.e., when  $0 < \Delta_T \ll 1$ ), the electric field  $E$  is always close to the breakdown value  $E_{br}$  and the discharge evolves very slowly.<sup>17</sup> Since the charge on the dielectric surface at the cathode grows as  $\dot{\sigma} = (1 + \gamma)j_{ic}$ , the change of the volume charge and the surface charge are connected according to the relationship

$$\dot{Q} = \frac{\Delta_T}{1 + \gamma} \dot{\sigma}. \tag{3}$$

Expanding  $\Delta_T$  in Taylor series near the breakdown, one can keep the first nonvanishing term:  $\Delta_T \approx \delta E (\partial \Delta_T / \partial E)$ , where  $\delta E \equiv E - E_{br}$ . Formula (3) shows that  $|Q| \ll |\sigma|$ , so that many generations of ions leave the gap and collect on the dielectric surface before the surface charge (and, hence, the electric field) change noticeably. In other words, the ions move in the adiabatically changing electric field, whose spatial distortion is negligible, and their spacial distribution has time to adjust to the instantaneous value of the field. Therefore, the rate of change of the volume charge,

$$\dot{Q} = \lambda Q, \tag{4}$$

is determined by the linear theory and can be evaluated as  $\lambda \sim \Delta_T (v_i / L)$ , where  $v_i$  is the ion drift velocity (see Appendix A, case  $\Delta_T \ll 1$ ). As ions (and electrons) collect on the dielectric, the surface charge increases causing the electric field in the gap to decrease:

$$\delta \dot{E} = -4\pi \dot{\sigma} / (1 + \epsilon L / 2d), \tag{5}$$

where  $2d$  is the total thickness of dielectric layers. In the course of time,  $E$  becomes smaller than the breakdown value  $E_{br}$ ,  $\Delta_T$  becomes negative and the discharge extinguishes. So, the discharge current first grows and then, after passing through the maximum, decreases; its time dependence can be readily found from the set of Eqs. (3)–(5):  $J(t) \propto \cosh^{-2}[1/2\lambda_{in}(t - t_m)]$ , where  $\lambda_{in}$  is the charge growth rate at the very beginning of the discharge and  $t_m$  is the moment

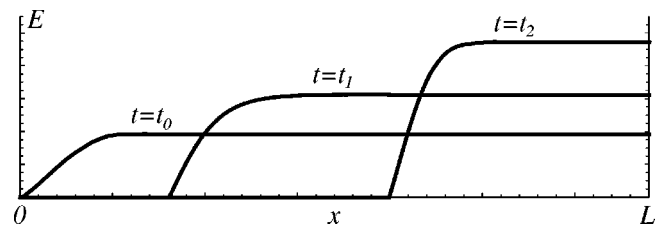


FIG. 2. Electric field at sequential time moments.

of the current maximum. The characteristic time of the current pulse is much greater than the ion transit time through the gap:  $\lambda_{in}^{-1} \sim (L/v_i) / \Delta_T (E_{in}) \gg L/v_i$ .

When the applied voltage significantly exceeds the breakdown voltage (i.e., when the parameter  $\Delta_T \gg 1$ ), one can expect that the discharge will evolve much faster. At the beginning, the charge in the gap does not affect the electric field and grows exponentially at a rate determined by the linear theory (see Appendix A, case  $\Delta_T \gg 1$ ):  $\lambda \approx (1 + \gamma) \alpha v_i$ . According to this formula, the amount of charge in the gap doubles as ions move only a small distance ( $\sim \alpha^{-1} \ll L$ ). For this reason, the ion distribution in the gap, roughly speaking, follows the distribution of their source; and because this source depends on the coordinate as  $\exp[\alpha(L-x)]$ , the bulk of the ions are accumulated near the anode (at the distance  $\sim \alpha^{-1}$ ). Note that during the linear stage, all of the electrons are quickly swept from the gap to the anode, and the negative charge in the gap can always be neglected.

Accumulation of the positive charge in the gap is accompanied by the decrease of the electric field in the small vicinity ( $\sim \alpha^{-1}$ ) of the anode. When the charge amount reaches the magnitude  $E_c / 4\pi$ , the electric field at the anode turns to zero. At this moment (which will be referred to as moment  $t_0$ ), the electric field near the cathode,  $E_c$ , still remains close to its initial value. If the growth of charge continued in the same way, the electric field near the anode would become negative (recall that, according to Gauss' law, the electric field at the anode,  $E_a = E_c - 4\pi Q$ ). The negative anode field blocks the passage of the electrons to the anode, which leads to their accumulation in the gap near the point of zero electric field. It means that, in the vicinity of the anode, the ion charge is compensated by the detained electrons, and the total charge in the gap stays at such a level that everywhere  $E \geq 0$ . Thus, from the moment  $t_0$ , the discharge dynamics undergoes a marked transformation—the electric field near the anode remains close to zero, and now there coexist two different regions in the gap: The neutral plasma region (plasma trail) with relatively small electric field, and the region of the gap adjacent to the cathode where the electric field is strong and the electron density is negligible (this region is called the CF region). The plasma trail expands toward the cathode and the CF region contracts with time (see Fig. 2) due to the continuing creation of plasma at the boundary of these regions. This process keeps going while the total charge in the CF region increases, i.e., while

$$\Delta_T \equiv \gamma \exp\left(\int_{CF} dx \alpha\right) - \gamma - 1 > 0. \tag{6}$$

When  $\Delta_T$  approaches zero, the dynamic CF either transforms into a quasi-dc CF or quickly disappears (see Sec. VI).

Let us illustrate the mechanism of the plasma trail expansion and the corresponding contraction of the CF region by considering a semihypothetical example when the ionization is caused by an external source (as it is in a nonself-sustained discharge; see, for example, Ref. 23). To further simplify the example, we assume that the power of the source is uniform throughout the gap,  $\dot{n}_i = \dot{n}_i(t)$ , the voltage across the gap is constant, the ion motion can be neglected, and the electrons leave the region of the strong electric field instantaneously. Under these conditions, the positive charge grows in the gap uniformly, and the electric field varies linearly with  $x$ :  $E(x, t) = V_a/L + 4\pi en_i(t)(x - L/2)$ . At the moment  $t_0$  when  $n_i(t_0) = V_a/2\pi eL$ , the anode electric field turns to zero. After that, the dividing point between the neutral plasma region and the region with uncompensated positive charge emerges from the anode and starts moving toward the cathode. As before, the electric field depends linearly on  $x$  in the uncompensated charge region, which allows one to obtain the relationship between the electric field on the cathode,  $E_c$ , the position of the dividing point (or front point),  $x_f$ , and the applied potential,  $V_a$ :  $1/2E_c(L - x_f) = V_a$ . By combining this equation with Gauss' law,  $E_c = 4\pi en_i(t)(L - x_f)$ , one can verify that, as the ion density grows, the region with nonzero field contracts according to the law  $(L - x_f) \propto n_i(t)^{-1/2}$ . The speed of this contraction is

$$\frac{\dot{x}_f}{\frac{1}{2}(L - x_f)} = \frac{P}{Q}, \tag{7}$$

where  $P = e\dot{n}_i(L - x_f)$  is the charge production and  $Q = en_i(L - x_f)$  is the charge in the  $E \neq 0$  region (per unit electrode area). This form of Eq. (7) emphasizes that the velocity of the dividing point is proportional to the production of charge in the electric-field region. Note, that this velocity is a finite quantity, although the ion velocity is zero and the electron velocity is infinite. The electron component of the current in the electric-field region increases linearly with distance from the cathode, reaching its maximum value at the dividing point,  $j_{e \max} = \dot{n}_i(L - x_f)$ , and it coincides in the plasma region with the total current  $J_{\text{tot}}/S = 1/4\pi\dot{E}_c = 1/2\dot{n}_i(L - x_f)$ , where  $S$  is the cross-sectional area of the discharge gap. A discontinuity of the electron current at the dividing point,  $\{j_e\} = j_{e \max} - J_{\text{tot}}/S = 1/2j_{e \max}$ , is connected with the process of plasma creation in the vicinity of the point  $x_f$ .

The dynamics of a barrier discharge is much more complicated: The particle production in the gap, caused by the electron ionization of the gas, is proportional to the ion flux to the cathode and is extremely inhomogeneous due to the avalanche nature of the ionization process. Almost all of the ions are produced at the end of the electron avalanche, so that the bulk of the uncompensated positive charge is concentrated in the small part ( $\Delta x_f \sim \alpha^{-1}$ , see Fig. 3) of the CF region immediately adjacent to the plasma trail. In the rest of the CF region, the amount of the charge is negligible and the electric field is approximately uniform,  $E(x, t) \approx E_c(t)$ . One

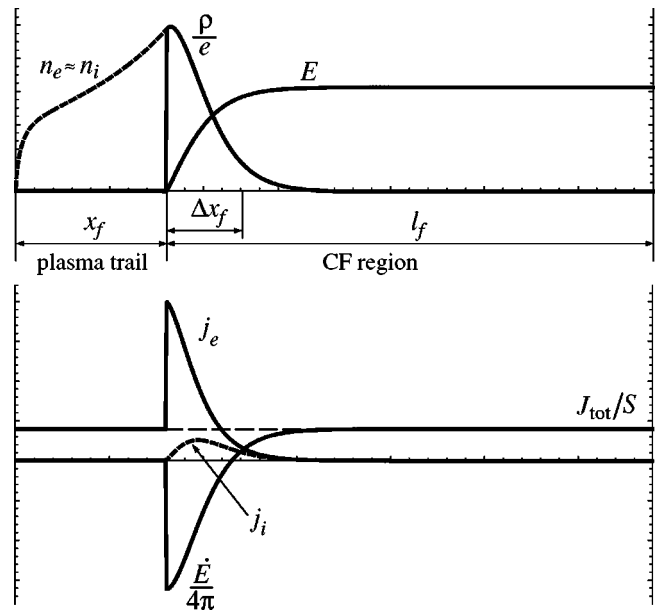


FIG. 3. Electric field and particle and current distributions across the gap in the discharge with  $\Delta_T \gg 1$ .

can say that the electric field in the gap has a steplike shape: It is close to zero in the plasma trail, and after a sharp increase, it is constant in the CF region.

So, while the ionization length  $\alpha^{-1}$  is small compared to the CF region length  $\ell_f$  ( $\ell_f \equiv L - x_f$ ), the expansion of the plasma region represents a propagation of the ionizing wave. This wave produces the positive charge on its front and then, after the compensation of this charge by the swept electrons, it leaves the plasma behind it, forming the expanding plasma trail. The plasma trail, considered as an element of the circuit, represents a conductor connecting the CF region with the anode. In this article, we will neglect the resistivity of the trail; the sharpness of the electric-field change will allow us to write a simple jump condition on the wave front, and the uniformness of the electric field in the CF region will simplify the evaluation of the ion density near the cathode (and by this way, the evaluation of the ion flux to the cathode).

Figure 3 exhibits two remarkable features of the spatial distribution of currents. First, the electron current experiences a jump at point  $x = x_f$ , because part of the electrons are “spent” on the creation of the plasma. To see this, let us present the total current in the gap as a sum of the ion and electron components and the displacement current,

$$J_{\text{tot}}(t) = \left( j_i + j_e + \frac{1}{4\pi} \dot{E} \right) S. \tag{8}$$

This representation, of course, follows from the charge continuity equation and the Poisson equation for the electric field. Averaging Eq. (8) over the CF region,  $x_f < x < L$ , and taking into account that  $\int_{x_f}^L dx (j_i + j_e) / \ell_f \sim (j_i + j_e)_{\max} \Delta x_f / \ell_f \sim j_{e \max} / \alpha \ell_f$  and  $\int_{x_f}^L dx \dot{E} / \ell_f = \dot{V}_{\text{gap}} / \ell_f < 0$ , we conclude that  $J_{\text{tot}}/S \sim j_{e \max} / \alpha \ell_f \ll j_{e \max}$ , i.e., the magnitude of the electron current at the left-hand side of point  $x = x_f$  is much less than at the right-hand side.

Second, the total current at the cathode is determined only by the displacement current,

$$J_{\text{tot}} \approx \frac{1}{4\pi} \dot{E}_c S. \quad (9)$$

The electron current from the surface of the cathode is proportional to the ion current to this surface,  $j_{ec}S = \gamma j_{ic}S$ , so that the particle current at the cathode is equal to  $(1 + \gamma)j_{ic}S$ . It can be neglected in comparison with the total current,  $J_{\text{tot}} \sim j_{e \text{ max}} S / \alpha \ell_f \sim (\gamma e^{\alpha \ell_f} / \alpha \ell_f) j_{ic}S$ , when  $(1 + \gamma) \ll \gamma e^{\alpha \ell_f} / \alpha \ell_f$ . Note that the behavior of the electric field in the CF region resembles the behavior of the electric field in a capacitor in which one plate moves toward the other.

### III. BASIC EQUATIONS

We will study the propagation of the plane ionizing wave in the framework of the widely used fluid model.<sup>4</sup> In this model, the continuity equations for the electrons and ions are coupled with the Poisson equation:

$$-e \frac{\partial n_e}{\partial t} + \frac{\partial j_e}{\partial x} = -\alpha j_e, \quad (10)$$

$$e \frac{\partial n_i}{\partial t} + \frac{\partial j_i}{\partial x} = \alpha j_e, \quad (11)$$

$$\frac{\partial E}{\partial x} = 4\pi e(n_i - n_e), \quad (12)$$

where  $e$  is the elementary charge and  $n_e$  and  $n_i$  are the electron and ion densities, respectively. The electron and ion current densities in the drift-diffusion approximation are

$$j_e = en_e \mu_e E + e D_e \frac{\partial n_e}{\partial x}, \quad (13)$$

$$j_i = en_i \mu_i E, \quad (14)$$

where  $\mu_e$  and  $\mu_i$  are the ion and electron mobilities, and  $D_e$  is the electron diffusion coefficient. We have neglected the diffusion motion of the ions, because their average energy is always small. The voltage applied to the cell is divided between the gap and the dielectric layers which are charged by the current flowing in the circuit:

$$V_{\text{gap}} + \frac{q}{C} = V_a, \quad (15)$$

$$\frac{dq}{dt} = J_{\text{tot}}, \quad (16)$$

where  $C = \epsilon S / 8\pi d$  is the capacity of the layers. Hereafter, the applied voltage  $V_a$  is assumed to be constant.

In Sec. II, we have clarified that, as the ionizing wave propagates from the anode to the cathode, two regions can be clearly distinguished in the discharge gap: The expanding plasma trail and the contracting CF region. In the plasma region, adjacent to the anode, the electric field is close to zero,  $E \approx 0$ , the electron and ion densities are equal,  $n_e = n_i = n_p$  ( $n_p$  is the plasma density), and the current consists of a flow of electrons,  $J_{\text{tot}} = j_e S$ .

In the CF region, adjacent to the cathode, the electric field is strong and the electron density is negligible,  $n_e \approx 0$ . It allows us to express the ion and electron current densities in terms of the electric field. Substituting the ion density from the Poisson equation into Eq. (14) gives

$$j_i = \frac{1}{4\pi} \mu_i E E', \quad (17)$$

where prime means  $x$  derivatives. By neglecting the electron transit time through the CF region and taking into account that at the cathode  $j_e(L, t) = \gamma j_i(L, t) \equiv \gamma j_{ic}$ , we can obtain the electron current from Eq. (10):

$$j_e = \gamma j_{ic} \exp\left(\int_x^L dx \alpha\right). \quad (18)$$

A discontinuity of the electron current at the dividing point  $x_f$  results in the creation of plasma, whose density can be also determined from Eq. (10). Using that, in the vicinity of  $x_f$ , we can write  $\partial j_e / \partial x \approx \{j_e\} \delta[x - x_f(t)]$  [where  $\delta(x)$  is the Dirac delta function, and  $\{j\}$  is the magnitude of the electron current jump] and integrating Eq. (10) over a small time interval  $(t' - \delta t, t' + \delta t)$ , we find

$$n_p(x) = n_e(x) = \{j_e\} / \dot{x}_f(t'), \quad (19)$$

where  $t'$  is the moment when the dividing point  $x_f$  passes the point  $x$ .

To find a jump condition at the wave front and, by doing so, the front velocity, it is convenient to use Eq. (8). Substituting Eqs. (17) and (18) into Eq. (8), we obtain the equation for the electric field:

$$\dot{E} + \mu_i E E' + 4\pi \gamma j_{ic} \exp\left[\int_x^L dx \alpha(E)\right] = 4\pi J_{\text{tot}} / S, \quad (20)$$

where  $j_{ic} = en_{ic} \mu_i E_c$  and, according to Eq. (9),  $J_{\text{tot}} / S \approx \dot{E}_c / 4\pi$ . Multiplying Eq. (20) by  $\alpha(E)$ , integrating it from 0 to  $L$ , and using condition  $E(x < x_f) = 0$ , we obtain:

$$\dot{I} + \mu_i E_c \langle \alpha E \rangle_c + 4\pi \gamma j_{ic} (e^R - 1) = \dot{E}_c R, \quad (21)$$

where hereafter the angle brackets denote an average over the electric field,  $\langle f \rangle \equiv E^{-1} \int_0^E df$ ,  $\langle f \rangle_c \equiv \langle f \rangle|_{E=E_c}$ ;  $I \equiv \int_{x_f}^L dx E \langle \alpha \rangle$  and  $R \equiv \int_{x_f}^L dx \alpha$ . When  $E$  is close to a step function, we can calculate the integrals,  $I \approx \ell_f E_c \langle \alpha \rangle_c$  and  $R \approx \ell_f \alpha_c$ , and then find the difference between the first terms in left- and right-hand sides of Eq. (21):

$$\dot{I} - \dot{E}_c R \approx \langle \alpha \rangle_c E_c \dot{\ell}_f. \quad (22)$$

So, in the zeroth order of approximation in parameter  $(\alpha \ell_f)^{-1}$ , Eq. (21) takes the form

$$\langle \alpha \rangle_c \dot{x}_f \approx \mu_i \langle \alpha E \rangle_c + 4\pi en_{ic} \mu_i \gamma e^R, \quad (23)$$

where we took into account that  $\dot{\ell}_f = -\dot{x}_f$ . This equation can be written in the form that represents the charge balance in the ionizing wave [compare with Eq. (7)],

$$\frac{(\dot{x}_f - \bar{v}_i)}{\Delta x_f} \approx \frac{P}{Q}, \quad (24)$$

where  $\Delta x_f = \langle \alpha \rangle_c^{-1}$  is the characteristic size of the spatial localization of the positive charge and  $\bar{v}_i = \mu_i \langle \alpha E \rangle_c / \langle \alpha \rangle_c$  is an average ion velocity;  $P \approx \gamma e n_{ic} \mu_i E_c e^R$  is the rate of the charge production and  $Q = E_c / 4\pi$  is the amount of the positive charge in the CF region (per unit electrode area). The left-hand side term in Eq. (24) is inversely proportional to the time during which the wave “eats away” the positive charge in the CF region; the right-hand side term is proportional to the charge reproduction rate.

In deriving Eq. (23), we assume that the electron transit time is negligible, so that at each moment the electron avalanche develops in an almost stationary electric field. It takes place when

$$\frac{\Delta x_f}{\dot{x}_f} \gg \frac{\ell_f}{v_e} = \frac{\ell_f}{\mu_e E_c}. \quad (25)$$

In what follows, we will neglect, for simplicity, the voltage drop across the plasma region (that is justified providing that  $J_{tot}$  is not too large). In this case, one can easily find a connection between the electric field near the cathode,  $E_c$ , and the position of the ionizing wave front,  $x_f$ . Integrating Eq. (16) over time from 0 to  $t$  with  $J_{tot}/S$  from (9) gives:  $q/C = E_c L_v$  ( $L_v \equiv S/4\pi C = 2d/\epsilon$  is the width of the vacuum capacitor with capacitance  $C$ ). Substituting this result into Eq. (15) and keeping in mind that the voltage drop across the plasma region is negligible and the voltage drop across the CF region for a steplike electric field is approximately equal to  $E_c \ell_f$ , one obtains

$$E_c = \frac{V_a}{\ell_f + L_v}. \quad (26)$$

Differentiating this formula and using expression (23) for the front velocity lead to the equation for electric field  $E_c$ :

$$\dot{E}_c = \frac{\mu_i E_c \langle \alpha E \rangle_c + 4\pi \gamma j_{ic} e^R}{\langle \alpha \rangle_c (V_a / E_c)}, \quad (27)$$

where  $R \approx \alpha_c \ell_f$ .<sup>24</sup> Equation (27) confirms our qualitative assumption that the total current is always much smaller [in  $\langle \alpha \rangle_c V_a / E_c = \langle \alpha \rangle_c (\ell_f + L_v)$  times!] than the characteristic value of the particle current on the wave front.

In the case when the electron current from the cathode is controlled, for example, by externally induced photoemission and is a given function of time, one can integrate Eq. (27) and find the electric field and the position of the ionizing wave for any moment of time. However, in our case, this current is equal to  $\gamma j_{ic} \propto n_{ic}$  and one needs to supplement the equation for the electric field with the equation for the ion density near the cathode. In the plateau region, where the electric field  $E(x, t) = E_c(t)$ , the ion continuity equation takes the form

$$\dot{n}_i + v_{ic}(t) n_i' = \gamma \alpha_c(t) v_{ic}(t) n_{ic} e^{\alpha_c(t)(L-x)}, \quad (28)$$

where  $v_{ic}(t) = \mu_i E_c(t)$  and  $\alpha_c(t) = \alpha[E_c(t)]$ . As we will see below, the wave front velocity is always greater than the maximum ion velocity in the CF and therefore, all ions reaching the cathode during the wave propagation are created and move in the uniform electric field  $E_c(t)$ . So, Eq. (28), for the ions near the cathode, does not require a boundary

condition at the left-hand side (i.e., at  $x \approx x_f + \Delta x_f$ ).<sup>25</sup> The influence of the ionizing wave motion on the ion distribution in the plateau region comes only through the dependence of the electric field  $E_c$  on time. In this sense, the plateau region is disconnected from the front of the ionizing wave, where the electric field is substantially nonuniform.

In general, an accurate evaluation of the ion density depends on the rate of increase of  $E_c(t)$  with time. Nevertheless, one can show that the density growth rate can never exceed the one determined by the linear theory (see Appendix B):

$$\frac{\dot{n}_{ic}}{n_{ic}} \leq \lambda(t) = (1 + \gamma) \alpha[E_c(t)] \mu_i E_c(t). \quad (29)$$

In order to use Eqs. (28) and (29), we must know  $n_{ic}$  at the moment  $t_0$  when the electric field near the anode turns to zero and the ionizing wave starts to travel toward the cathode. The total charge in the gap at this moment is

$$Q = (E_c - E_a) / 4\pi \approx E_0 / 4\pi, \quad (30)$$

where  $E_0 \equiv V_a / (L + L_v)$ . On the other hand, since the ion distribution in the gap is still close to the one during the linear stage, the total charge can be estimated as  $Q \approx e n_{ic} \gamma e^R / \alpha(1 + \gamma)$  [see Eq. (A8) in Appendix A]. This estimate, in combination with Eq. (30), gives

$$n_{ic}(t_0) \xi = \frac{(1 + \gamma) \alpha_0 E_0}{4\pi e \gamma e^{R(t_0)}}, \quad (31)$$

where  $\alpha_0 \equiv \alpha(E_0)$ , and  $\xi \sim 1$  is the numerical factor introduced to account for the distortion of the electric field near the anode [the specific value of this factor depends on the behavior of the function  $\alpha(E)$  in the vicinity of the point  $E = E_0$ ]. Taking into account Eq. (31), one finds the wave velocity at the moment  $t_0$ :

$$\langle \alpha \rangle_c \dot{x}_f \approx \mu_i \langle \alpha E \rangle_c + (1 + \gamma) \mu_i \alpha_c E_c \xi^{-1}. \quad (32)$$

#### IV. IONIZING WAVE BETWEEN BARE ELECTRODES

In this section, we will assume that the dielectric layers are so thin that  $L_v = S/4\pi C = 2d/\epsilon$  is always much smaller than the CF region length  $\ell_f$  and the total voltage drop across these layers is negligible. From Eq. (26), it follows that  $E_c \approx V_a / \ell_f$  and the parameter  $R$  on the right-hand side of Eqs. (23) and (27) is approximately

$$R \approx \alpha_c \ell_f \approx \eta(E_c) V_a, \quad (33)$$

where the ionization coefficient  $\eta(E) \equiv \alpha(E)/E$ . Since the charge production in the gap is proportional to the exponential factor  $e^R$ , the wave velocity strongly depends on how the function  $\eta(E)$  varies with  $E$ . As we will see below, there are two qualitatively different regimes of the propagation of the ionizing wave: (1) The fast regime which takes place when the factor  $e^R$  increases as the wave advances toward the cathode ( $d\eta/dE > 0$ ), and (2) the slow regime which is realized when  $e^R$  decreases ( $d\eta/dE < 0$ ).

##### A. Fast regime: Increasing function $\eta(E)$

In order to reveal the distinctive features of this regime, we suppose that the ionization coefficient  $\eta(E)$  is an increas-

ing function for all values of  $E$ ,  $0 \leq E < \infty$ . In this case, the parameter  $R$  increases as the ionizing wave moves toward the cathode and, therefore, the wave front becomes steeper and steeper. It means that our approximation of the electric field by a steplike function [ $E(x, t) = 0$  for  $0 \leq x \leq x_f$  and  $E(x, t) \approx E_c(t)$  for  $x_f \leq x \leq L$ ] only improves when the wave approaches the cathode. Since the wave velocity grows, the ionizing wave quickly reaches the cathode and the CF region collapses. As a matter of fact, the CF contracts so fast that the ion density at the cathode remains bounded up to the moment of the collapse (although the electric field and the total amount of charge in the CF region grow without limit  $E_c = V_a / (L - x_f) \rightarrow \infty$  when  $x_f \rightarrow L$ ;  $Q = E_c / 4\pi \rightarrow \infty$ ). To show this, let us divide Eq. (29) by Eq. (27):

$$\frac{dn_{ic}}{dE_c} \leq \frac{(1 + \gamma)\alpha_c \mu_i E_c n_{ic} \langle \alpha \rangle_c (V_a / E_c)}{\mu_i E_c \langle \alpha E \rangle_c + 4\pi e n_{ic} \mu_i E_c \gamma e^R}. \quad (34)$$

Omitting the first term in the denominator on the right-hand side of Eq. (34) (that only strengthens this inequality) and integrating over  $E_c$  leads to the expression:

$$\delta n_{ic} \leq \frac{(1 + \gamma)}{4\pi e \gamma} V_a \int_{E_{in}}^{V_a / \ell_f} dE \frac{\alpha \langle \alpha \rangle e^{-\eta V_a}}{E}, \quad (35)$$

where  $\delta n_{ic}$  is the change of the ion density during the time in which the wave front moves from the initial position ( $x_f = 0$ ) to the current position ( $x_f = L - \ell_f$ ) and  $E_{in} \approx V_a / L$ . For a very broad class of increasing functions  $\eta(E)$ , the integral on the right-hand side of Eq. (35) converges when its upper limit tends to infinity, which means that the ion density near the cathode remains bounded.

For illustration, let us consider the propagation of the ionizing wave when  $\eta \propto E^s$ ,  $s \geq 1$  (such a shape of the ionization coefficient greatly simplifies the calculations). Performing the integration in Eq. (35), omitting small terms  $\sim R^{-1}$ , and then taking into account Eq. (31), one can obtain the estimate for the maximum change of the ion density near the cathode:

$$\max \delta n_{ic} \leq \frac{(1 + \gamma)\alpha_0 \langle \alpha \rangle_0}{4\pi e \gamma s \eta_0 e^{\eta_0 V_a}} = \frac{n_{ic} \xi}{s(1 + s)}, \quad (36)$$

where the subscript 0 refers to the initial moment  $t_0$ . It turns out that in the case  $s \geq 1$ , the numerical coefficient  $\xi$  is quite small so that the ion density  $n_{ic}$  remains almost constant from the start of the propagation of the wave to its collapse. According to Eq. (32), at the initial moment  $t_0$ , the second term on the right-hand side of Eq. (23) is already significantly greater than the first term, and due to its exponential growth it dominates all the time as the wave moves from the anode to the cathode. Neglecting the ion motion on the wave front, one obtains the following equation for the wave velocity and the electric field:

$$\dot{x}_f = 4(1 + s)\pi e n_{ic} \mu_i \alpha_c^{-1} \gamma e^R, \quad (37)$$

$$\dot{E}_c = 4(1 + s)\pi e n_{ic} \mu_i E_c \frac{\gamma e^R}{R}, \quad (38)$$

where  $R = \eta(E_c)V_a$ , and we used the equality  $\langle \alpha \rangle = \alpha / (1 + s)$ . The result of the integration of these equations over time is

$$x_f = L - L \left( 1 - \frac{1}{R_0} \ln \frac{t_* - t}{\Delta t_*} \right)^{-1/s}, \quad (39)$$

$$E_c(t) = \frac{V_a}{L} \left( 1 - \frac{1}{R_0} \ln \frac{t_* - t}{\Delta t_*} \right)^{1/s}, \quad (40)$$

$$\Delta t_* = \frac{1}{12\pi e n_{ic} \mu_i \gamma e^{R_0}} = \frac{\langle \alpha \rangle_0^{-1}}{\dot{x}_{f0}}, \quad (41)$$

where  $t_* = t_0 + \Delta t_*$  is the moment when the collapse of the ionizing wave occurs. Since the wave rapidly accelerates (its speed increases more than  $e^s$  times as the wave passes the distance  $\alpha^{-1}$ ), it spends most of its time moving through the small initial part of the path [ $\langle \alpha \rangle_0^{-1} \ll L$ ].

We can summarize the features of this regime as follows: The wave front becomes steeper and steeper as the ionizing wave moves toward the cathode; the CF region collapses and the electric field becomes infinite in finite time  $\Delta t_*$ ; the ion density near the cathode remains bounded (or even almost constant) during this time; the wave front velocity increases with time so fast that  $\dot{x}_f / v_i \rightarrow \infty$ .

If  $\eta(E)$  is a very slow growing or decreasing function of  $E$  then, as one can see from Eq. (35), there is no limitation on the growth of the ion density at the cathode. A characteristic example of the wave propagation with simultaneously growing the density  $n_{ic}$  and the electric field  $E_c$  is described in Sec. IV B.

## B. Slow regime: Decreasing function $\eta(E)$

When  $\eta(E)$  is a decreasing function, the parameter  $R$  decreases and the ratio of the wave front length to the CF region length grows as the ionizing wave moves toward the cathode. The difference between the front and the plateau becomes less and less pronounced with time and eventually, when  $\Delta_T$  approaches zero, the dynamic CF transforms into a regular dc CF.

First, we consider the propagation of the ionizing wave when the function  $\alpha(E) = \text{constant}$  ( $\eta \propto E^{-1}$ ), which corresponds to the behavior of the ionization coefficients  $\alpha$  and  $\eta$  at strong electric fields. In this case, Eq. (28) for the ion density in the plateau region has the exact solution

$$n(x, t) = n_0 \exp \left[ \int_{t_0}^t dt \lambda(t) - \alpha x \right], \quad (42)$$

where  $\lambda(t)$  depends on time through the electric field  $E_c$ :  $\lambda(t) = (1 + \gamma)\alpha \mu_i E_c(t)$ . As seen from Eq. (42), the ion density near the cathode grows with the rate  $\lambda(t)$ . The initial value of this density,  $n_0 \equiv n_{ic}(t_0)$ , is given by expression (31), in which we must again put  $\xi = 1$  (during the transition period  $R = \alpha L = \text{constant}$ ). By using this expression, Eq. (23) for the front velocity can be written as

$$\frac{\dot{x}_f}{\mu_i E_c} = \frac{1}{2} + (1 + \gamma) \frac{E_0}{E_c} \frac{n_{ic}}{n_0} e^{\alpha \ell_f}, \quad (43)$$

where we used that  $\langle \alpha E \rangle_c = \alpha E_c / 2$  for  $\alpha = \text{constant}$ . Differentiating Eq. (43) with respect to time and using the equalities  $\dot{n}_{ic} = \lambda n_{ic}$  and  $\dot{E}_c = \dot{x}_f E_c / \ell_f = \dot{x}_f \alpha E_c / R$ , one can obtain the equation for the ratio  $\dot{V}_f = \dot{x}_f / \mu_i E_c$ :

$$\frac{d}{dt} \tilde{V}_f = \lambda \left( \tilde{V}_f - \frac{1}{2} \right) \left( 1 - \frac{1+R^{-1}}{1+\gamma} \tilde{V}_f \right), \quad (44)$$

where  $R = \alpha \ell_f$ . Equation (44) shows that, after a time of the order of  $\lambda^{-1}$ , the ratio of the front velocity to the ion velocity becomes close to its asymptotic value:

$$\frac{\dot{x}_f}{\mu_i E_c} = \frac{1+\gamma}{1+R^{-1}} \approx 1 + \gamma. \quad (45)$$

This result has a simple interpretation. Since the second term on the right-hand side of Eq. (43) contains one sharply increasing factor  $n_{ic}/n_0 = \exp[\int_0^t dt \lambda(t)]$  and one sharply decreasing factor  $e^R$ , the wave velocity can be found from the condition of “phase” constancy:

$$\lambda + \frac{d}{dt} R = 0. \quad (46)$$

Equation (46) leads to Eq. (45) when  $R = \alpha \ell_f$  and  $\lambda = (1 + \gamma) \alpha \mu_i E_c$ . As the wave front moves toward the cathode and the plateau region length  $\ell_f = L - x_f$  becomes smaller, the electric field grows,  $E_c = V_a / \ell_f$ , and the wave front accelerates,  $\dot{x}_f \approx (1 + \gamma) \mu_i V_a / (L - x_f)$ . Solving the last equation, one can find the time that it takes the wave to cross the gap and approach the cathode:

$$\Delta t_* \approx \frac{L^2}{2(1 + \gamma) \mu_i V_a}.$$

When  $\ell_f$  becomes of the order of the dc CF length  $\ell_{CF} \sim \alpha^{-1} \ln(1 + \gamma^{-1})$ , the parameter  $\Delta_T$  approaches zero, and the CF region can no longer be divided into a front region and a plateau region. In a short time ( $\sim \ell_{CF}^2 / \mu_i V_a \ll \Delta t_*$ ), the dynamic CF transforms into a dc CF (more precisely, into a quasi-dc CF, see Sec. VI).

The electric field in the case  $\alpha = \text{constant}$  ( $\eta \propto E^{-1}$ ) grows relatively slowly,  $\dot{E}_c / E_c \sim \dot{x}_f / \ell_f \sim \lambda / R$ , so that

$$\frac{\dot{E}_c}{E_c} \ll \frac{\dot{n}_{ic}}{n_{ic}}. \quad (47)$$

It turns out that this inequality holds true in a more general case of decreasing function  $\eta(E)$ . For a slowly changing electric field, the function  $\alpha_c(t)$  in Eq. (28) changes adiabatically slowly with time, and the solution of this equation is still given by Eq. (42). Therefore,  $\dot{n}_{ic} \approx \lambda n_{ic}$ . Substituting  $R = \eta(E) V_a$  into Eq. (46), one can obtain the wave front velocity for the more general case:

$$\frac{\dot{x}_f}{\mu_i E_c} = \frac{(1 + \gamma) \alpha_c}{E_c^2 |d\eta/dE_c|}. \quad (48)$$

Here, it was assumed that the function  $\eta(E)$  decreases not too slowly:  $\alpha_c^{-1} E_c^2 |d\eta(E_c)/dE_c| \gg R^{-1}$ ; so that the small terms in the denominator could be omitted.

The intermediate case  $\eta(E) = \text{constant}$  requires a special treatment [we cannot use Eq. (48) because its right-hand side now goes to infinity]. When  $\eta$  is constant, the parameter  $R$  is also constant and, thus, the length of the wave front with respect to the entire length of the CF region remains unchanged. The latter fact suggests that Eq. (20) admits a self-similar solution:

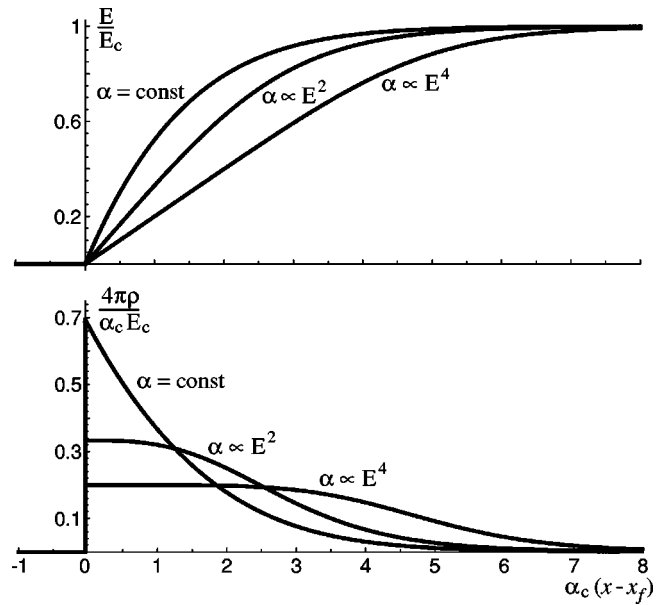


FIG. 4. Electric-field and charge density distributions on the front of the ionizing wave.

$$E(x, t) = \frac{1}{\sqrt{t_* - t}} \mathcal{E} \left( \frac{L - x}{\sqrt{t_* - t}} \right),$$

$$E_c \propto \frac{1}{\sqrt{t_* - t}}, \quad n_{ic} \propto \frac{1}{t_* - t}.$$

The relative wave velocity in this regime  $\tilde{V}_f \equiv \dot{x}_f / \mu_i E_c = \text{constant} < R$ .

### V. CHARGE AND PLASMA DISTRIBUTIONS

We already mentioned above that almost all positive charge is localized in the narrow layer within the ionizing wave front,  $x_f < x < x_f + \Delta x_f$ . To describe the structure of this front, let us return to the basic equation (20). First, note that in the region of the wave front, the total current is small compared to the particle current,  $J_{\text{tot}}/S \sim (j_e + j_i) / \langle \alpha \rangle \ell_f \ll j_e + j_i$ , and can be neglected. Second, the displacement current in this region is caused mostly by the front motion:  $\dot{E} \approx -\dot{x}_f E'$ . After these simplifications, Eq. (20) takes the form

$$-\dot{x}_f E' + \mu_i E E' + 4\pi e \gamma j_{ic} e^{R(x)} = 0, \quad (49)$$

where  $R(x) \equiv \int_x^L dx \alpha$ . Multiplying this equation by  $\alpha$  and then performing the spatial integration from  $x_f$  to  $x$ , we obtain

$$-\dot{x}_f \langle \alpha \rangle E + \mu_i \langle \alpha E \rangle E + 4\pi \gamma j_{ic} [e^{R(x_f)} - e^{R(x)}] = 0. \quad (50)$$

Using Eqs. (50) and (23), we can express  $e^{R(x)}$  in terms of the known functions  $\langle \alpha \rangle$  and  $\langle \alpha E \rangle$ . Substituting the result into Eq. (49) and regrouping the terms lead to the equation

$$(\dot{x}_f - \mu_i E) E' = \langle \alpha (\dot{x}_f - \mu_i E) \rangle_c E_c - \langle \alpha (\dot{x}_f - \mu_i E) \rangle E,$$

whose solution can be easily expressed in quadratures. The shape of the wave front for different functions  $\alpha = \alpha(E)$  is pictured in Fig. 4.

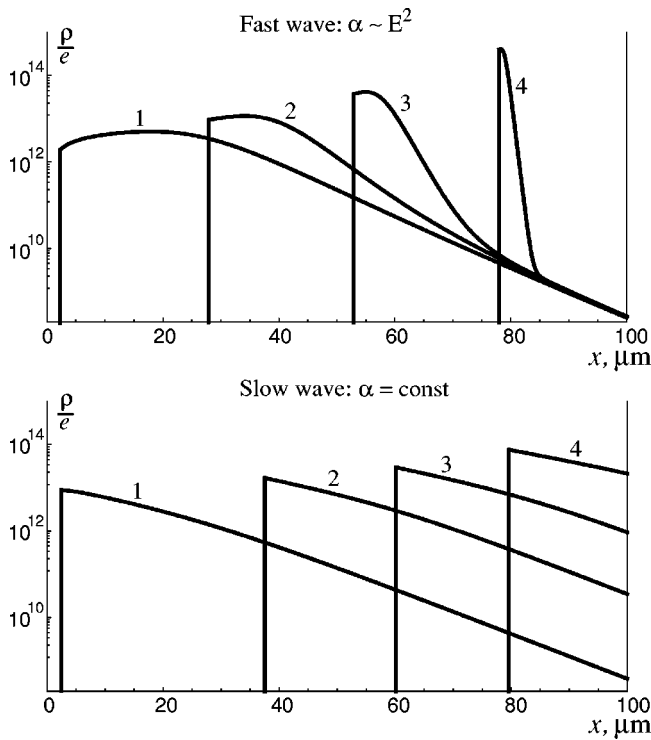


FIG. 5. Charge density distribution across the whole discharge gap at sequential time moments.

Figure 4 also illustrates the distribution of the positive charge density,  $\rho = E' / 4\pi e$ , within the wave front. This density turns to zero at the point  $x = x_f$  in accordance with the fact that the region  $x < x_f$  is occupied by the neutral plasma. Figure 5 helps one get an idea of how the positive charge is distributed over the whole CF region in the different regimes of the wave propagation. Let us note that in the fast regime, the charge density on the wave front grows independently of the charge density at the cathode, whereas in the slow regime they change synchronously.

As we discussed above, the electrons created in the CF region are swept from this region into the plasma trail. The major portion of these electrons goes to compensate for the positive charge; that leads to formation of the plasma trail right behind the wave front. Taking into account Eqs. (19) and (23), the expression for the plasma density can be written as

$$n_p(x) = \frac{1}{4\pi e} \langle \alpha \rangle_c E_c (1 - \delta), \tag{51}$$

where

$$\delta \equiv \frac{\mu_i \langle \alpha E \rangle_c}{\langle \alpha \rangle_c \dot{x}_f} = \frac{\bar{v}_i}{\dot{x}_f},$$

depends on the coordinate  $x$  through the electric field:  $E_c = V_a / (L - x)$ . It can be shown that  $\delta \leq 0.5$ : If  $\alpha$  grows with  $E$  faster than a linear function then  $\dot{x}_f \gg \bar{v}_i$  and  $\delta \approx 0$ ; If  $\alpha$  is constant then  $\dot{x}_f \approx 2(1 + \gamma)\bar{v}_i$  and  $\delta = 0.5 / (1 + \gamma)$ . The plasma density always grows with the distance from the anode. For example,  $n_p(x) \propto 1 / (L - x)^{1+s}$  ( $0 < x < x_f$ ) when  $\alpha \propto E^s$ .

## VI. IONIZING WAVE BETWEEN ELECTRODES WITH DIELECTRIC LAYERS

In this section, we consider the barrier discharge when the voltage drop across the dielectric layers has a perceptible effect on its dynamics. Regarding the ionization coefficients, we assume that  $\alpha(E)$  and  $\eta(E)$  are typical functions of the electric field for real gases. For definiteness, we will use the following simple formula for the ionization coefficient:<sup>23</sup>

$$\alpha(E) = \alpha_{\max} e^{-E_{\text{norm}}/E}. \tag{52}$$

For pure Ne gas under the pressure  $P = 500$  Torr, the coefficient  $\alpha_{\max} = 4P = 2 \times 10^3 \text{ cm}^{-1}$  and  $E_{\text{norm}} = 100P = 5 \times 10^4 \text{ V/cm}$ . In all of the examples below, the secondary electron emission coefficient  $\gamma = 0.64$ .

We can picture both dielectric layers as one piece of the dielectric with the vacuum permeability and the effective length  $L_v = 2d/\epsilon$  which is adjacent to the cathode electrode, so that the whole distance between the anode and cathode electrodes is equal to  $L + L_v$ . This representation allows one to conclude immediately that if there is only a positive charge in the gas gap and on the dielectric surface, then the electric field monotonically increases from the anode to the cathode. Hence, the capacitor imposes a limitation on the maximum attainable value of the electric field in the gap:

$$E_c \leq (V_a - V_{\text{gap}}) / L_v \leq E_* \equiv V_a / L_v.$$

In the steplike approximation (when the charge is localized only on the wave front), the electric field stays uniform throughout the CF region and the “vacuum” capacitor as the ionizing wave moves toward the cathode, so that  $E_c(\ell_f + L_v) = V_a$ .

If the gas gap is long enough and the initial electric field in the gap  $E_{\text{in}}$  is so strong that the parameter  $R = \alpha(E_{\text{in}})L \gg 1$ , the ionizing wave forms near the anode and then starts moving toward the cathode. The propagation of this wave is governed by Eq. (27), where the parameter  $R \approx \alpha_c \ell_f \approx \alpha_c (V_a / E_c - L_v) \approx \bar{\eta}(E_c) V_a$  is determined by the modified function  $\bar{\eta}(E) = \eta(E)(1 - E/E_*)$ .

Depending on the strength of  $E_{\text{in}}$ , two qualitatively different cases are possible. In the first case, when the initial electric field lies within the range corresponding to the growing part of  $\bar{\eta}(E)$  function (i.e., when  $E_{\text{in}} = E_1 < \bar{E}_m$ , see Fig. 6), the ionizing wave quickly accelerates as was described in the Sec. IV A. According to Eq. (35), the ion density near the cathode changes insignificantly, as long as the current value of the parameter  $R$  is greater than its initial value. In other words,  $n_{ic} \approx n_{ic}(t_0)$  while  $E_1 < E_c < E_2$  [see Fig. 7(a)]. In this range, the total current is entirely determined by the charge production term which is proportional to  $e^R$  [see Eq. (27)]. It reaches its first maximum at almost the same value of the electric field as the factor  $e^{\bar{\eta}(E_c)V_a}$  does:  $E_c \approx \bar{E}_m$ . The other maximum is reached at the high electric field when the ionizing wave approaches the cathode [see Fig. 7(b) showing the currents versus the wave front position].

In the second case, when the initial electric field lies in the range corresponding to the falling part of  $\bar{\eta}(E)$  function (i.e., when  $E_{\text{in}} = E_2 > \bar{E}_m$ ), the growth of the ion density near the cathode balances the drop of the factor  $e^R$  so that the

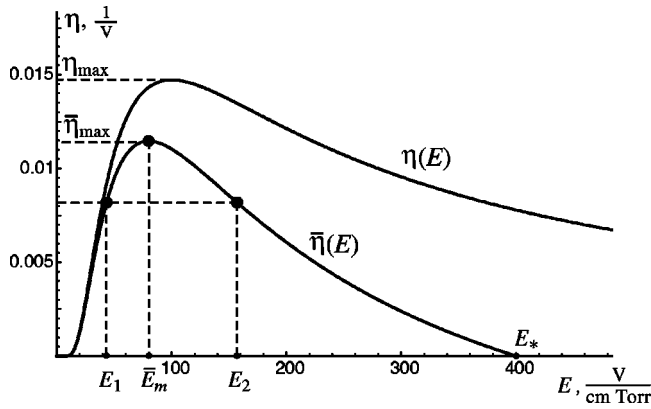


FIG. 6. Typical shape of  $\eta(E)$  and corresponding  $\bar{\eta}(E)$  for  $V_a=1200$  V and  $L_v=60$   $\mu\text{m}$ .

ionizing wave moves with the velocity given by Eq. (48) in which  $\eta$  should be substituted by  $\bar{\eta}$ . The total current grows monotonically (while the parameter  $\Delta_T$  is great enough) and can be evaluated by

$$\frac{J_{\text{tot}}}{S} = \frac{E_c^2 \dot{x}_f}{4\pi V_a} = \frac{(1+\gamma)\mu_i E_c \alpha_c}{4\pi V_a |d\bar{\eta}/dE_c|}. \quad (53)$$

It is worth noting that in both cases, the ionizing wave has the same characteristics on the common part of its path. In Fig. 7(b) is also shown the current for the intermediate case when the initial electric field is equal to  $\bar{E}_m$ ; it behaves similarly to the current in the  $E_{\text{in}} > \bar{E}_m$  case. The time dependence of the currents for the considered cases is shown in Fig. 8.

When the CF region length becomes so small that the parameter  $\Delta_T$  approaches zero, the difference between the front and the plateau region disappears and our approxima-

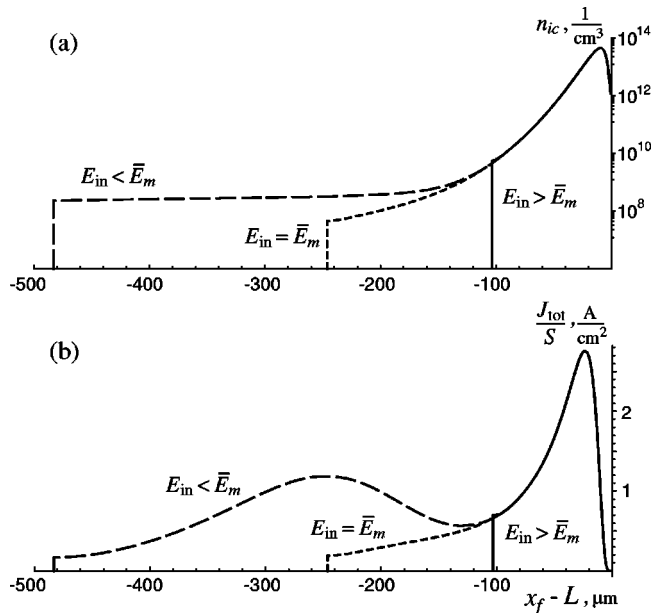


FIG. 7. Ion density  $n_{ic}$  and  $J_{\text{tot}}$  vs  $x_f - L$  for different  $E_{\text{in}}$  and the same  $V_a=1200$  V and  $L_v=60$   $\mu\text{m}$ . The gap length  $L \approx 482$   $\mu\text{m}$  for  $E_{\text{in}}=E_1 < \bar{E}_m$ ,  $L \approx 245$   $\mu\text{m}$  for  $E_{\text{in}}=\bar{E}_m$ , and  $L \approx 102$   $\mu\text{m}$  for  $E_{\text{in}}=E_2 > \bar{E}_m$ . In these cases,  $\alpha(E_{\text{in}})L$  is 11, 14, and 11, respectively.

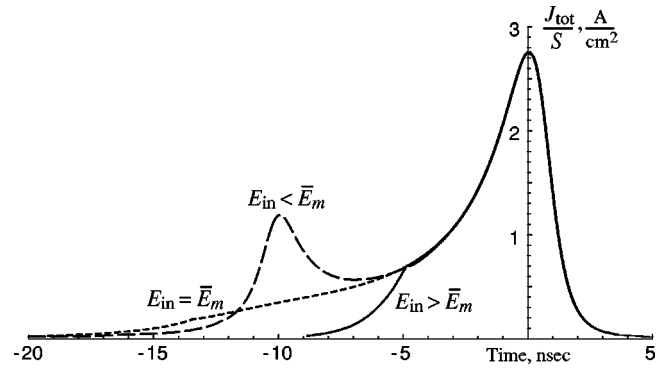


FIG. 8.  $J_{\text{tot}}$  vs  $t$  for different  $E_{\text{in}}$  and the same  $V_a=1200$  V and  $L_v=60$   $\mu\text{m}$ . (Time is measured from the moment of the common maximum of the currents.)

tion is no longer valid. What happens next depends on how the applied voltage is divided between the dielectric layer and the CF region.

First, let us compare the applied voltage  $V_a$  with the normal CF voltage,<sup>23</sup>  $V_{\text{norm}} \approx \ln(1+\gamma^{-1})/\eta_m$ , where  $\eta_m$  is the maximum value of the ionization coefficient  $\eta(E)$ . Since  $\eta_m V_a \geq \bar{\eta}_m V_a \geq R_{\text{max}}$ , where  $R_{\text{max}}$  is the maximum value of the parameter  $R$  during the discharge, we obtain the inequality

$$\frac{V_a}{V_{\text{norm}}} \geq \frac{R_{\text{max}}}{\ln(1+\gamma^{-1})}. \quad (54)$$

One can see from Eq. (54) that the applicability condition for our approximation ( $R \gg 1$  at the beginning of the discharge) is satisfied only when the applied voltage is much greater than the normal voltage.

When the effective length of the capacitor is much smaller than the CF region length,  $L_v \ll \ell_{\text{CF}}$ , the dynamic CF transforms into the quasi-stationary dc CF. The initial voltage across it is close to the applied voltage,  $V_{\text{CF}} \approx V_a$ , and since  $V_a \gg V_{\text{norm}}$ , this CF is abnormal; its length can be evaluated as

$$\ell_{\text{CF}} \approx \ell_{\text{abn}}, \quad \ell_{\text{abn}} = \alpha_{\text{max}}^{-1} \ln(1+\gamma^{-1}).$$

The quasi-stationary CF produces the current,  $J_{\text{tot}} \approx S(1+\gamma)\mu_i V_{\text{CF}}^2/4\pi\ell_{\text{CF}}^3$ , which charges the capacitor:  $\dot{q} = J_{\text{tot}}$ . On the other hand,  $(4\pi L_v/S)q + V_{\text{CF}} = V_a$ . Combining these equalities, we obtain the equation for the time variation of the CF voltage

$$\frac{\dot{V}_{\text{CF}}}{L_v} \approx -(1+\gamma) \frac{\mu_i V_{\text{CF}}^2}{\ell_{\text{CF}}^3}, \quad (55)$$

where  $\ell_{\text{CF}}$  now depends on the instant value of the CF voltage and is determined by the relationship

$$\alpha(V_{\text{CF}}/\ell_{\text{CF}})\ell_{\text{CF}} = \ln(1+\gamma^{-1}). \quad (56)$$

According to Eq. (55), the voltage across the CF decreases with a characteristic time  $t_{\text{CF}} \sim (\ell_{\text{CF}}/L_v)\tau_i$ , much greater than the ion transit time through the CF region,  $\tau_i \sim \ell_{\text{CF}}/v_i \sim \ell_{\text{CF}}^2/\mu_i V_{\text{CF}}$ . It means that, at nearly the same voltage  $V_{\text{CF}}$ , many generations of ions replace each other in the CF, and their distribution in space has time to become almost station-

ary. When the voltage across the CF drops to the normal CF voltage  $V_{\text{norm}}$ , the CF starts to decay, sharply decreasing the charge production. However, to fully charge the capacitor it is still necessary to put the charge  $CV_{\text{norm}}$  on its plates. If the capacitor is large enough, the decaying CF will extract all the ions from the plasma trail. At the end, there will be a uniform residual electric field in the gap.

So, when the effective length of the capacitor is much smaller than the abnormal CF length ( $L_v \ll \ell_{\text{abn}}$ ), the picture of the discharge dynamics appears as follows: (1) the ionizing wave originates at the anode and propagates toward the cathode, then (2) the ionizing wave transforms into a quasi-dc CF, which charges the capacitor, and (3) as the discharge decays, the region with the residual electric field expands backward, toward the anode.

The ionizing wave charges the capacitor only to a small voltage  $\sim (L_v/\ell_{\text{CF}})V_a$ ; most of the capacitor voltage builds up during the charging by the quasi-stationary dc CF. The decaying CF further charges the capacitor increasing its voltage by the amount less than or equal to  $V_{\text{norm}}$ .

Let us note that our consideration is not quite correct because the typical currents produced by the dc CF are large and the voltage drop across the plasma trail is significant. Nevertheless, one can always distinguish three stages in the discharge dynamics: Ionizing wave, quasi-stationary dc CF, and decaying CF.

In the case when the effective length of the capacitor is comparable to the abnormal CF length ( $L_v \sim \ell_{\text{abn}}$ ), the significant part of the applied voltage drops across the capacitor at the moment when the parameter  $\Delta_T$  approached zero. Although the electric field in the CF region is much greater than  $E_{\text{norm}}$ , the capacitor is charged by a few generations of ions, and therefore no quasi-dc CF forms. In the case of a large effective length of the capacitor ( $L_v \gg \ell_{\text{abn}}$ ), the capacitor is almost fully charged during the propagation of the ionizing wave. After the moment when the parameter  $\Delta_T$  becomes zero, the ions are deposited on the dielectric surface, and the CF region quickly disappears. Thus, after the discharge, there is no residual electric field in the gap.

In conclusion of this section, let us consider the limiting case when the vacuum length  $L_v \rightarrow \infty$  ( $C=0$ ), while the initial electric field in the gap is kept constant. Since the charge on the capacitor does not change during the discharge ( $\delta q = C \delta V \equiv 0$ ,  $\delta V \leq V_{\text{gap}}$ ), the total current in the circuit is identically equal to zero. This system is equivalent to the one with very thin dielectric layers over the electrodes which were initially charged to voltage  $V_{\text{gap}}$  and then disconnected from the voltage source. Now, the charge on the electrodes remains constant as the discharge develops. While the parameter  $\Delta_T$  is large, the electric field within the plateau region does not change with time ( $\dot{E}_c \approx 4\pi J_{\text{tot}}/S \equiv 0$ ), neither does the ionization coefficient. Using the results of Sec. IV B, we find that the ionizing wave moves with a constant velocity  $\dot{x}_f = (1 + \gamma)\mu_i E_c$  and passes through the gap in time  $\Delta t_* = L/\dot{x}_f$ . The voltage between the electrodes decreases uniformly in time to zero,  $V_{\text{gap}} = E_c L(1 - t/\Delta t_*)$ . Let us note that in contrast to the case of small  $L_v$ , neglecting the voltage drop across the plasma trail is well justified now because the current  $J_{\text{tot}} \equiv 0$ .

## VII. DISCUSSION

Let us discuss applicability and some generalizations of obtained results.

- (1) The presented theory is applicable to strong barrier discharges ( $\Delta_T \gg 1$ ), when the length of the discharge gap is much longer than the length of the normal CF and the voltage applied to the gap is considerably greater than the breakdown voltage. In such discharges,  $pL$  and  $V_{\text{gap}}$  are relatively large, so that the operating point ( $pL, V_{\text{gap}}$ ) lies above the right-hand side branch of the Pashen curve.

Note that although in all examples we used to illustrate the barrier discharge dynamics in Sec. VI (see Fig. 7), the lengths of the discharge gap and initial voltages across the gap are quite different, all operating points belong to the aforementioned region in the  $pL - V_{\text{gap}}$  plane. It is appropriate to note here that in strong barrier discharges, current densities limited by the dielectric capacitance can be quite small.

- (2) Our consideration can be generalized to include the series resistor  $R$  in the external circuit. In this case, Eqs. (23), (28), and (29) remain valid, and Eq. (26) must be replaced by

$$E_c = \frac{V_a - J_{\text{tot}}R}{\ell_f + L_v} = \frac{V_a - \frac{1}{4\pi} \dot{E}_c SR}{\ell_f + L_v}. \quad (57)$$

Note that now Eq. (27) for the electric field must be modified.

- (3) In this work, we neglected the resistance of the plasma trail and the transit time of electrons through the CF region, i.e., we assumed, in essence, the electron mobility infinite. Taking into account the effects of the finite electron mobility results in the decrease of the discharge current. The case when the plasma trail plays a crucial role in the dynamics of the barrier discharge will be considered in our future work.
- (4) Although  $\gamma$  and  $\mu_i$  were constant, one can easily generalize our theory to the case when  $\gamma = \gamma(E)$  and  $\mu_i = \mu_i(E)$ . One can also include in our analytical consideration the case when the discharge gap is filled with a mixture of gases.
- (5) We found that dynamics of a barrier discharge in plane geometry strongly depends on the ratio of the effective length of the dielectric layer capacitor  $L_v = 2d/\epsilon$  to the length of the dc CF. We think that this ratio determines, to a large extent, the discharge behavior in more complicated geometries.
- (6) One of the interesting predictions of the presented theory (that, to our knowledge, has not been observed experimentally) is that the discharge current under certain conditions may have two maxima rather than one (see Fig. 8). To make sure that this feature of a strong barrier discharge is not the result of simplifications used in our analysis, we compare the time dependence of the discharge current obtained from the presented model with that obtained under the same conditions from the more accurate drift-diffusion model (described by Eqs. (10)–

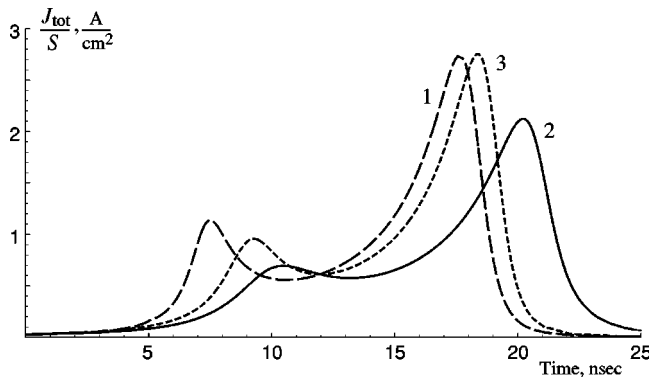


FIG. 9. Dependence of the discharge current on time: (1) is obtained from the presented simplified model ( $V_a=1200$  V,  $L_v=60$   $\mu\text{m}$ , and  $L \approx 482$   $\mu\text{m}$ ); (2) is obtained from the drift-diffusion model (the same discharge parameters); and (3) is obtained from the drift-diffusion model when the total voltage across the CF region and the dielectric layers is kept constant.

(16), wherein the electron diffusion coefficient  $D_e = \mu_e T_e$  and the electron temperature  $T_e$  was about several electron volts). As it is seen from Fig. 9, in the drift-diffusion model, the discharge develops more slowly and current peaks are smaller (compare curves 1 and 2). When we purposely keep the total voltage across the CF region and the dielectric layer constant, and by doing so, eliminate the effect of the finite resistance of the plasma trail, the difference between the models is greatly diminished (see curve 3 in Fig. 9).

### VIII. CONCLUDING REMARKS

We have shown that at high overvoltage, the barrier discharge takes the form of an ionizing wave originating at the anode and propagating toward the cathode. The wave characteristics depend on the behavior of the parameter  $\Delta_T$  (which equals the number of extra ions created by the electron avalanche which results from one ion striking the cathode):

- (1) When the parameter  $\Delta_T$  grows with the advance of the ionizing wave, the CF region contracts so quickly that the ion density near the cathode remains almost unchanged. The wave velocity in this regime can be considerably greater than the ion velocity;
- (2) When the parameter  $\Delta_T$  decreases, the CF region contracts relatively slowly so that the ion density near the cathode increases many times while the electric field changes insignificantly. In this regime, the wave velocity is close to the ion velocity.

Under certain conditions, the discharge goes sequentially through both regimes, and the discharge current  $J_{tot}(t)$  may experience two maxima. The first one occurs, roughly speaking, at the moment when the charge production rate in the CF region reaches its maximum (i.e., when the parameter  $\Delta_T$  is maximum). The second one occurs when the electric field in the CF region reaches its maximum (i.e., when the parameter  $\Delta_T$  is close to zero and the length of the CF region is of the order of the dc CF length).

The discharge dynamics is quite sensitive to the magnitude of the capacitor formed by the dielectric layers. When the capacitance is large, the ionizing wave propagates as in the case without the capacitor. Reaching the cathode, the wave transforms into the quasi-dc CF, which almost fully charges the capacitor. When the capacitance is small, it significantly influences the characteristics of the ionizing wave. Reaching the cathode, the wave quickly disappears and no quasi-dc CF forms.

### APPENDIX A: LINEAR THEORY

When the charge in the gap is small, the electric field can be considered uniform and constant. In this approximation, electron current (18) takes the form

$$j_e = \gamma j_{ic} e^{\alpha(L-x)}. \tag{A1}$$

Now ion continuity equation (11) can be written as

$$e \frac{\partial n_i}{\partial t} + \frac{\partial j_i}{\partial x} = \alpha \gamma j_{ic} e^{\alpha(L-x)}, \tag{A2}$$

where, according to Eq. (14),  $n_i = j_i / e \mu_i E \equiv j_i / e v_i$ . Making a substitution  $j_i \rightarrow j_i(x) e^{\lambda t}$ , we obtain the following equation for the ion current density:

$$\frac{dj_i}{dx} + \frac{\lambda}{v_i} j_i = \alpha \gamma j_{ic} e^{\alpha(L-x)}. \tag{A3}$$

Multiplying Eq. (A3) by  $e^{\lambda x/v_i}$ , and integrating it over the gap with boundary conditions on the anode,  $j_i(0) = 0$ , and on the cathode,  $j_i(L) = j_{ic}$ , we find the equation for growth rate  $\lambda$ :

$$\frac{e^{\xi} - 1}{\xi} = \frac{1}{\alpha L \gamma}, \quad \xi \equiv \left( \alpha - \frac{\lambda}{v_i} \right) L. \tag{A4}$$

When the parameter  $\Delta_T = \gamma(e^{\alpha L} - 1) - 1 \ll 1$ , from Eq. (A4) follows that the increment is much smaller than the inverse ion transit time,

$$\lambda \approx a \Delta_T (v_i/L), \tag{A5}$$

where constant

$$a = \left[ 1 + \gamma - \frac{1}{\ln(1 + \gamma^{-1})} \right]^{-1}.$$

In the opposite case when  $\Delta_T \gg 1$  [more exactly, when  $\alpha L \gg \ln(1 + \gamma^{-1})$ ], the increment is

$$\lambda \approx (1 + \gamma) \alpha v_i. \tag{A6}$$

The distribution of the ion density in the gap is

$$n_i(x) = \gamma \alpha_c L n_{ic} e^{\alpha_c(L-x)} \frac{e^{\xi(x/L)} - 1}{\xi}. \tag{A7}$$

Integrating Eq. (A7) over  $x$  from 0 to  $L$  gives the total charge in the gap:  $Q = \Delta_T e n_{ic} v_i / \lambda$ . For  $\Delta_T \gg 1$ , this expression takes the form

$$Q \approx \frac{\Delta_T}{1 + \gamma} e n_{ic} \alpha^{-1} \approx \frac{\gamma e^R}{1 + \gamma} e n_{ic} \alpha^{-1}. \tag{A8}$$

## APPENDIX B: ESTIMATE FOR GROWTH RATE OF ION DENSITY AT THE CATHODE

Integrating Eq. (28) along the characteristics and neglecting the initial ion density in the gap, we obtain the following integral equation for the ion density near the cathode:

$$n_{ic}(t) = n_{i0}[x(t, t_0)] + \gamma \int_{t_0}^t dt' \Omega(t') n_{ic}(t') e^{\psi(t, t')}, \quad (\text{B1})$$

where  $n_{i0}(x)$  is the ion density at the moment  $t_0$  when the ionizing wave starts to travel toward the cathode,  $x(t, t') = L - \int_{t'}^t dt'' v_{ic}(t'')$  is the coordinate of the ion at the moment  $t'$ , reaching the cathode at the moment  $t$ ,  $\Omega(t') \equiv \alpha_c(t') v_{ic}(t')$ , and  $\psi(t, t') \equiv \alpha_c(t') [L - x(t, t')]$ . Taking the time derivative of (B1) gives

$$\begin{aligned} \dot{n}_{ic}(t) = & -v_{ic}(t) n'_{i0}[x(t, t')] + \gamma \alpha_c(t) v_i(t) n_{ic}(t) \\ & + \gamma v_i(t) \int_{t_0}^t dt' \alpha_c(t') \Omega(t') n_{ic}(t') e^{\psi(t, t')}. \end{aligned} \quad (\text{B2})$$

At time moment  $t_0$ , the distribution of the ion density near the cathode is still described by the linear theory. Using Eq. (A7), one can find an estimate

$$|n'_{i0}(x)| \leq \alpha_c(t_0) n_{i0}(x). \quad (\text{B3})$$

Taking into account inequality  $\alpha_c(t') \leq \alpha_c(t)$  and Eqs. (B3) and (B1), from (B2) follows

$$\begin{aligned} \dot{n}_{ic}(t) \leq & \alpha_c(t_0) v_{ic}(t) n_{i0}(x) + \gamma \alpha_c(t) v_i(t) n_{ic}(t) \\ & + v_i(t) \alpha_c(t) [n_{ic} - n_{i0}(x)] \\ \leq & (1 + \gamma) \alpha_c(t) \mu_i E_c(t) n_{ic}(t). \end{aligned}$$

- <sup>1</sup>D. Braun, U. Kuchler, and G. Pietsch, *J. Phys. D* **24**, 564 (1991).
- <sup>2</sup>Z. Falkenstein and J. Coogan, *J. Appl. Phys.* **82**, 6273 (1997).
- <sup>3</sup>U. Reitz, J. G. Salge, and R. Schwarz, *Surf. Coat. Technol.* **59**, 144 (1993).
- <sup>4</sup>J. Meunier, P. Belenguer, and J. P. Boeuf, *J. Appl. Phys.* **78**, 731 (1995).
- <sup>5</sup>C. Punset, J. P. Boeuf, and L. C. Pitchford, *J. Appl. Phys.* **83**, 1884 (1998).
- <sup>6</sup>C. Punset, S. Cany, and J. P. Boeuf, *J. Appl. Phys.* **86**, 124 (1999).
- <sup>7</sup>P. J. Drallos, V. N. Khudik, and V. P. Nagorny, in *Proceedings of SID'98* (Anaheim, CA, 1998), pp. 632–635.
- <sup>8</sup>R. Veerasingam, R. B. Campbell, and R. T. McGrath, *IEEE Trans. Plasma Sci.* **24**, 1399 (1996).
- <sup>9</sup>R. Veerasingam, R. B. Campbell, and R. T. McGrath, *Plasma Sources Sci. Technol.* **6**, 157 (1997).
- <sup>10</sup>S. Raju and M. J. Kushner, *J. Appl. Phys.* **85**, 3460 (1999).
- <sup>11</sup>S. Raju and M. J. Kushner, *J. Appl. Phys.* **85**, 3470 (1999).
- <sup>12</sup>G. J. M. Hagelaar, M. H. Klein, R. J. M. M. Snijders, and G. M. W. Kroesen, *J. Appl. Phys.* **89**, 2033 (2001).
- <sup>13</sup>Y. Ikeda, J. P. Verboncoeur, P. J. Christenson, and C. K. Birdsall, *J. Appl. Phys.* **86**, 2431 (1999).
- <sup>14</sup>Y. Ikeda, K. Suzuki, H. Fukumoto, J. P. Verboncoeur, P. J. Christenson, C. K. Birdsall, M. A. Shibata, and M. A. Ishigaki, *J. Appl. Phys.* **88**, 6216 (2000).
- <sup>15</sup>G. Veronis, U. S. Inan, and V. P. Pasko, *Appl. Phys. Lett.* **78**, 25 (2001).
- <sup>16</sup>Y. Murakami, H. Matsuzaki, H. Murakami, and K. Tachibana, *Jpn. J. Appl. Phys., Part 1* **39**, 590 (2000).
- <sup>17</sup>V. P. Nagorny, P. J. Drallos, and W. Williamson, Jr., *J. Appl. Phys.* **77**, 3645 (1995).
- <sup>18</sup>V. I. Kolobov and A. Fiala, *Phys. Rev. E* **50**, 3018 (1994).
- <sup>19</sup>I. Brauer, C. Punset, H. G. Purwins, and J. P. Boeuf, *J. Appl. Phys.* **85**, 7569 (1999).
- <sup>20</sup>M. C. Wang and E. E. Kunhardt, *Phys. Rev. A* **42**, 2366 (1990).
- <sup>21</sup>N. W. Albright and D. A. Tidman, *Phys. Fluids* **15**, 86 (1972).
- <sup>22</sup>R. F. Fernsler, *Phys. Fluids* **27**, 1005 (1983).
- <sup>23</sup>Y. P. Raizer, *Gas Discharge Physics* (Springer, Berlin, 1991).
- <sup>24</sup>It is necessary to note that our approximation allows one to determine the front coordinate  $x_f$  with accuracy  $\Delta x_f \sim \alpha_c^{-1}$  and the parameter  $R$  with accuracy  $\Delta R \sim 1$ . By more accurately calculating the electric-field distribution in the ionizing wave (see Sec. V), in principle, we can improve the accuracy of our consideration.
- <sup>25</sup>Note that in contrast to the dynamic CF in a dc CF, all of the ions, regardless of where they are created, reach the cathode. Therefore, in order to determine the ion density near the cathode, one has to solve the ion continuity equation in the entire CF region.